

*to be published in Astronomy Letters, 2016, v. 42, pp. 69-81*

## X-RAY NOVA MAXI J1828–249. EVOLUTION OF THE BROADBAND SPECTRUM DURING ITS 2013–2014 OUTBURST

S.A. Grebenev<sup>1\*</sup>, A.V. Prosvetov<sup>1</sup>, R.A. Burenin<sup>1</sup>,  
R.A. Krivonos<sup>1</sup>, and A.V. Mescheryakov<sup>1,2</sup>

<sup>1</sup>*Space Research Institute, Russian Academy of Sciences, Profsoyuznaya ul.  
84/32, Moscow, 117997 Russia*

<sup>2</sup>*Kazan Federal University, Kremlevskaja ul. 18, Kazan, 420008 Russia*

Submitted on June 5, 2014

Based on data from the SWIFT, INTEGRAL, MAXI/ISS orbital observatories, and the ground-based RTT-150 telescope, we have investigated the broadband (from the optical to the hard X-ray bands) spectrum of the X-ray nova MAXI J1828–249 and its evolution during the outburst of the source in 2013–2014. The optical and infrared emissions from the nova are shown to be largely determined by the extension of the power-law component responsible for the hard X-ray emission. The contribution from the outer cold regions of the accretion disk, even if the X-ray heating of its surface is taken into account, turns out to be moderate during the source’s “high” state (when a soft blackbody emission component is observed in the X-ray spectrum) and is virtually absent during its “low” (“hard”) state. This result suggests that much of the optical and infrared emissions from such systems originates in the same region of main energy release where their hard X-ray emission is formed. This can be the Compton or synchro-Compton radiation from a high-temperature plasma in the central accretion disk region puffed up by instabilities, the synchrotron radiation from a hot corona above the disk, or the synchrotron radiation from its relativistic jets.

**DOI:** 10.1134/S1063773716020031

**Keywords:** *X-ray sources, transients, black holes.*

---

\* E-mail: <sergei@hea.iki.rssi.ru>

## INTRODUCTION

The outburst of the previously unknown X-ray transient MAXIJ1828–249 at  $\sim 1^\circ 5'$  from the accreting pulsar 4U 1826–24 was detected by the GSC/MAXI instrument on October 15, 2013, at 21<sup>h</sup>55<sup>m</sup> UT (Nakahira et al. 2013). By the time of the discovery, the photon flux from the source reached  $\sim 90$  mCrab in the 2–10 keV energy band; the spectrum was soft, a blackbody one. The position of the transient in the sky, initially determined with an accuracy of  $\sim 0''.3$ , was improved during its observation with the IBIS/ISGRI telescope of the INTEGRAL observatory (Filippova et al. 2013) and, subsequently, with the XRT and UVOT telescopes of the SWIFT observatory (Kennea et al. 2013a, 2013b):  $R.A.(J2000) = 18^h28^m58^s.07$  and  $Dec.(J2000) = -25^\circ01'45''.88$  (the uncertainty is  $0''.03$ ). The source turned out to be faint in the ultraviolet,  $M2 \simeq 18.6$ . Given the very moderate absorption measured in its X-ray spectrum,  $N_H \sim 2 \times 10^{21} \text{ cm}^{-2}$ , it can be attributed to low-mass X-ray binaries. The photon flux from the source in the 20–80 keV energy band was  $\sim 45$  mCrab, while its spectrum was hard, a power law with a photon index  $\alpha \sim 1.7$  (Filippova et al. 2013). This result can be brought into agreement with the measurements of Nakahira et al. (2013) at low energies only by assuming that the source has a two-component spectrum similar to the spectra of X-ray novae<sup>1</sup> in their bright state (see, e.g., Sunyaev et al. 1988, 1991; Tanaka and Shibazaki 1996; Grebenev et al. 1997; Remillard and McClintock 2006; Cherepashchuk 2013). The subsequent observations performed on October 17–18 with the SWIFT and INTEGRAL observatories (Krivonos and Tsygankov 2013) showed that the source’s spectrum rapidly softened ( $\alpha \gtrsim 2$ ), which is also typical of X-ray novae on their way to maximum light. The radio observations made on October 18 with the Australian ATCA telescope revealed no emission from the source (Miller-Jones 2013). Note that the absorption measured in the source’s spectrum corresponded to the expected Galactic one in this direction,  $N_H \simeq (1.7 \pm 0.2) \times 10^{21} \text{ cm}^{-2}$  (Kalberla et al. 2005).

Thus, already the first days of observations showed that an X-ray nova flared up in the Galactic center region, and we had a unique chance to investigate the properties of yet another representative of the so far small population of these interesting objects and to test the existing theoretical models of disk accretion onto a black hole in a binary system. In this paper, we present the results of our monitoring of the nova outburst by the INTEGRAL (Winkler et al. 2003), MAXI (Matsuoka et al. 2009), and SWIFT (Gehrels et al. 2004) international astrophysical observatories. We use the publicly accessible data and the INTEGRAL data obtained within the Russian quota of observing time.

Of particular interest to us was the evolution of the broadband spectrum for this nova and primarily the properties of its optical, infrared (OIR), and ultraviolet (UV) emissions.

---

<sup>1</sup>Low-mass X-ray binaries containing a black hole that usually do not emit X-rays but occasionally flare up due to nonstationary accretion.

It is generally believed that such an emission appears in low-mass X-ray binaries due to the irradiation and heating of the outer cold accretion disk by X-ray photons from its hot central zone (Lyuty and Sunyaev 1976). However, recent studies of the broadband spectra for several X-ray novae, XTE J1118+480 (Chaty et al. 2003), MAXI J1836–194 (Grebenev et al. 2013), and SWIFT J174510.8–26241 (Grebenev et al. 2014), in their hard spectral state have shown that the OIR and UV emissions from these sources are an extension of the power law observed in the X-ray band and contain no clear evidence of a thermal emission component from the outer disk regions (see also Poutanen and Veledina 2014). Observations of the X-ray nova MAXI J1828–249 can give additional information for investigating this question.

## INSTRUMENTS AND DATA ANALYSIS

The data from the ISGRI detector (Lebrun et al. 2003) of the IBIS gamma-ray telescope (Ubertini et al. 2003) onboard the INTEGRAL observatory obtained within the Russian quota of observing time and in public access programs were used to study the outburst of this source. This detector is sensitive in the energy range 18–200 keV. Unfortunately, during the observations being discussed, the source never fell within the field of view of the INTEGRAL JEM-X monitor (Lund et al. 2003), which is narrower (with a diameter of  $13^{\circ}2$ ) than that of the IBIS telescope ( $30^{\circ} \times 30^{\circ}$ ).

At the SWIFT observatory, we used data from the BAT gamma-ray telescope sensitive in the energy range 15–150 keV with a field of view of 1.4 sr (Barthelmy et al. 2005), the XRT telescope sensitive in the energy range 0.2–10 keV (Burrows et al. 2005), and the UVOT optical and ultraviolet telescope sensitive in the range 170–600 nm (Roming et al. 2005). To obtain the sky images and to study the properties of individual sources, coded-aperture masks are used in the IBIS and BAT telescopes and grazing-incidence mirrors are used in the XRT telescope. We analyzed the data from all SWIFT telescopes using the standard data processing software packages (see also Evans et al. 2010 and references therein). The IBIS/ISGRI data were processed using the software developed at the Space Research Institute of the Russian Academy of Sciences (see, e.g., Revnivtsev et al. 2004; Krivonos et al. 2010). Our spectral analysis was performed with the NASA/HEASARC/XSPEC software package (Arnaud et al. 1996).

In the MAXI experiment onboard the International Space Station (ISS), we used data from the Gas Slit Camera (GSC) sensitive in the energy range 2–30 keV and scanning the entire sky every 90 min (Mihara et al. 2011). We used only the automatically processed light curves from the site MAXI.RIKEN.JP/TOP averaged on a scale of one day.

The optical and infrared observations of the source were performed with the Russian-Turkish 1.5-m telescope (RTT-150) on November 9–12, 2013. The detector was the TFOSC

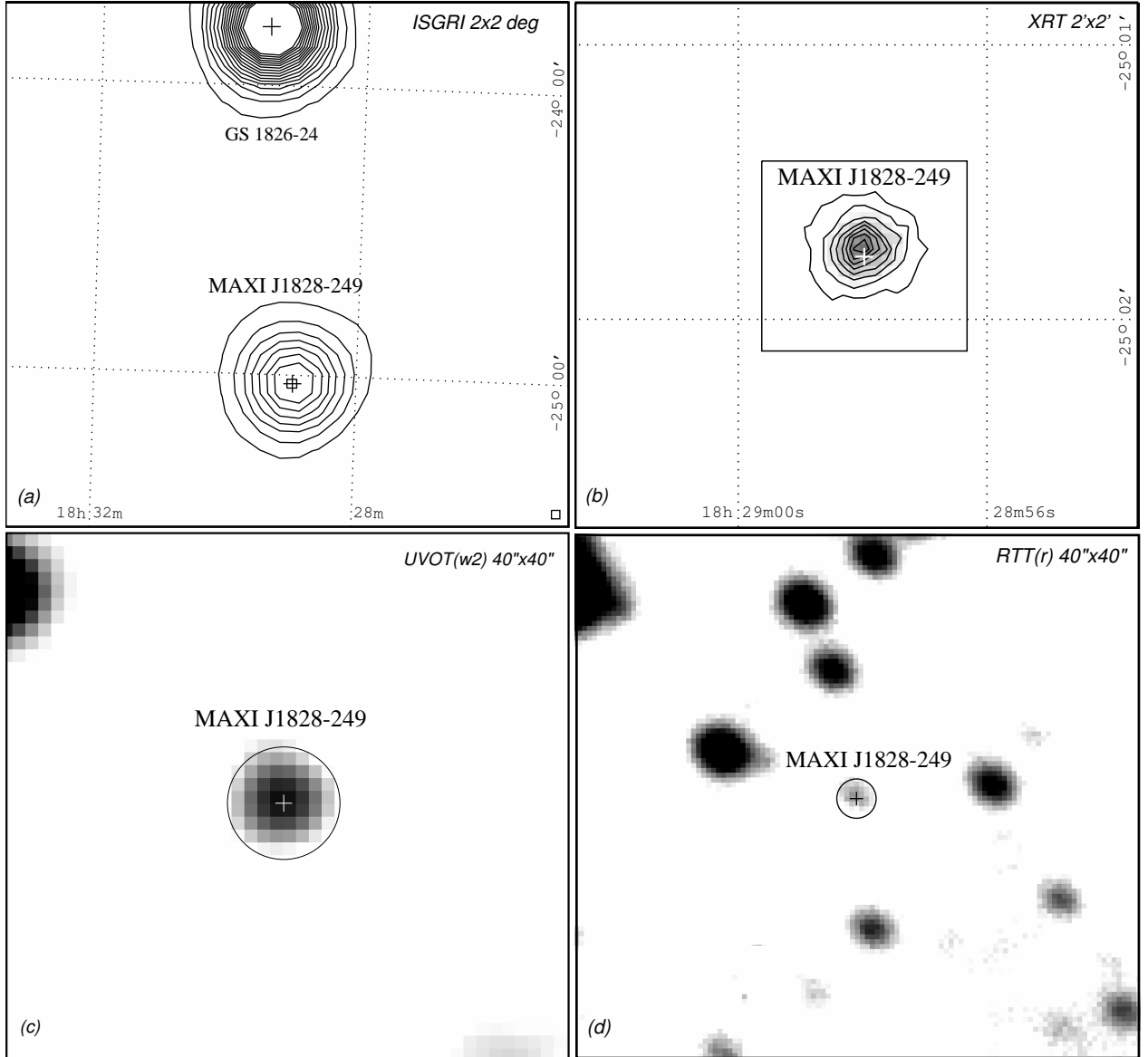
spectrometer, which operated for these measurements in the regime of a photometer in the  $v$ ,  $b$ ,  $z$ ,  $i$ ,  $r$ , and  $g$  filters, each with an exposure time of 60 s. We performed the photometric calibration using standard stars and processed the observations using the IRAF software package.

## RESULTS

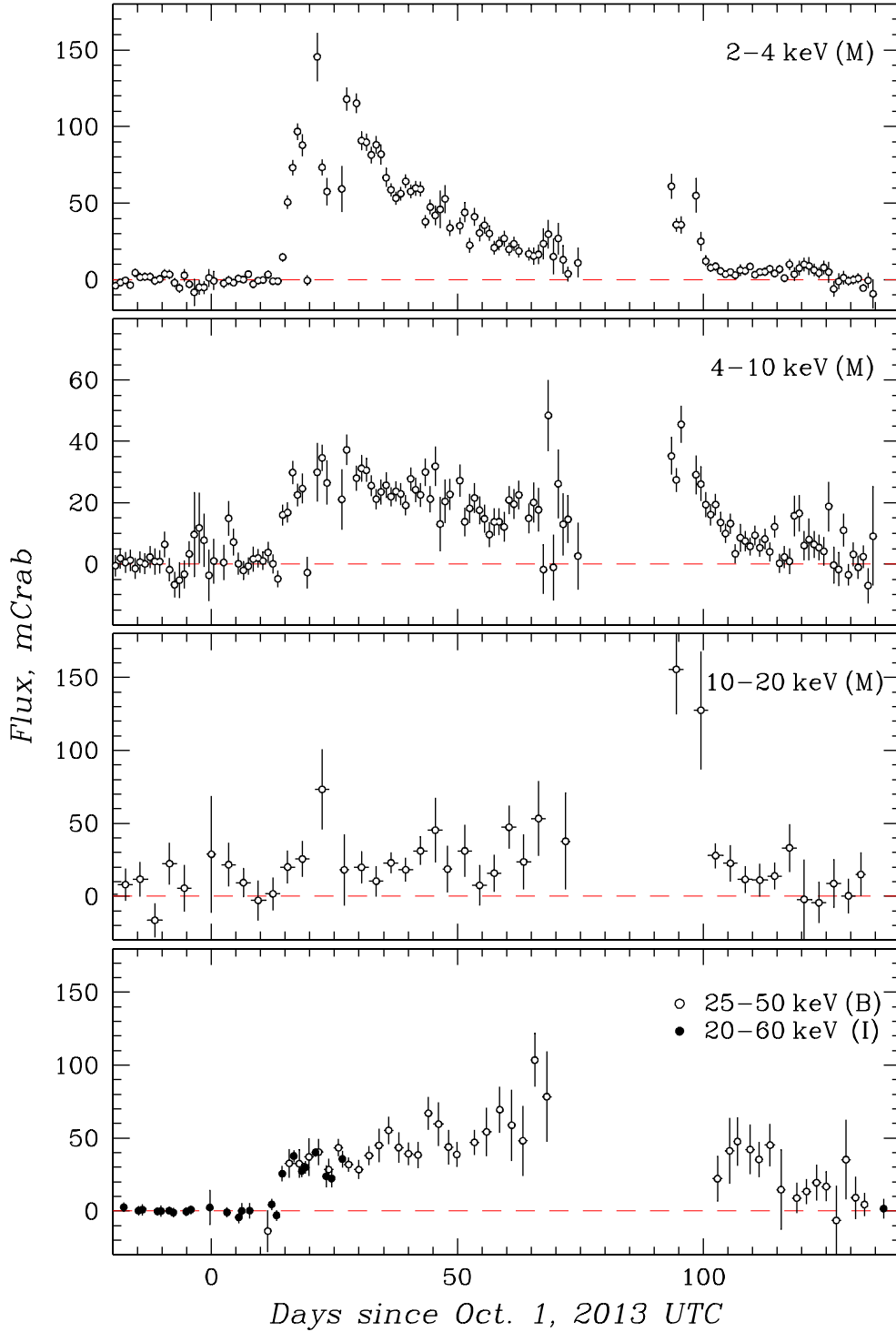
The IBIS/ISGRI/INTEGRAL, XRT and UVOT/SWIFT, and RTT-150 images of the sky region in which MAXI J1828–249 flared up are presented in Fig. 1. The images are given in order ( $a \rightarrow b \rightarrow c \rightarrow d$ ) of improving angular resolution of the telescopes (from  $12'$  for IBIS/ISGRI to  $\sim 2''$  for RTT-150; in the latter case, the average seeing is specified). The figure shows an ordinary path that has to be traversed from the detection of a new source by a wide-field X-ray telescope to its highly accurate optical localization. Owing to the moderate absorption and confident detection of MAXI J1828–249 in the ultraviolet (with the UVOT telescope, Fig. 1*c*), its accurate position was determined faster and easier than is usually done, when the identification of a transient in a crowded OIR field requires a meticulous analysis of the variability of all the infrared sources falling within it (Fig. 1*d*).

Figure 2 shows the light curve of the source constructed in four successive energy bands in the range from 2 to 60 keV from the MAXI, SWIFT, and INTEGRAL data. The light curve spans the period from the discovery of the transient (on October 15, 2013) to the end of February 2014. In the soft 2–4 keV X-ray band, the outburst of the transient has a FRED shape with a fast ( $\sim 5$  days) rise to  $\sim 100$ – $150$  mCrab and a slow ( $\sim 50$  days) exponential decay typical of X-ray novae. The second, much fainter outburst of the source began  $\sim 50$  days later, which is also typical of novae (the so-called “knee” in their light curves). Unfortunately, 5–10 days after the onset of the second outburst, the sky region with the source was no longer observable; therefore, we know little about the second outburst. After the resumption of observations in January 2014, the flux in soft X-ray bands (especially in the 4–10 keV band) was still appreciably higher than that before the onset of the second outburst. Note the short ( $\sim 10$  days) dip by  $\sim 40$ – $50\%$  in the 2–4 keV light curve observed shortly after maximum light. A similar dip was observed previously in the light curve of another X-ray nova, MAXI J1836–194 (Grebenev et al. 2013), and was explained by the transition of the source to a harder spectral state in the standard X-ray band, which is probably associated with the disappearance of the soft blackbody spectral component (or a noticeable decrease in its temperature).

In the hard ( $\gtrsim 20$  keV) X-ray band, the flux from the source after its sharp rise on October 15, 2013, to  $\sim 40$  mCrab subsequently changed gradually, showing a slow rise to  $\sim 60$  mCrab within the first two months after the outburst and a succeeding equally slow decay to  $\sim 40$  mCrab. The flux dropped abruptly by a factor of  $\sim 4$  in  $\sim 100$  days after the



**Fig. 1:** Images of the sky region near MAXI J1828–249 obtained with the IBIS/ISGRI telescope of the INTEGRAL observatory (20–60 keV), XRT (0.3–10 keV) and UVOT (W2 filter) telescopes of the SWIFT observatory, and the 1.5-m RTT-150 telescope (r filter). The  $S/N$  map is shown in the case of IBIS/ISGRI, and the intensity map is shown in the remaining cases. The images are given in order of improving angular resolution of the telescopes:  $12'$ ,  $5''$ ,  $2''.5$ , and  $\sim 2''$  (seeing). Their size decreases accordingly:  $2^\circ \times 2^\circ$ ,  $2' \times 2'$ , and  $40'' \times 40''$  (for the UV and IR images). The region in the UV and IR images is marked by the square in the XRT image; in turn, the XRT region is marked by the small square in the ISGRI image (for clarity, its size is also shown in the lower right corner of this image). The radius of the circumferences in the UV and IR images is  $4''$  and  $2''.5$ , respectively.



**Fig. 2:** X-ray light curve of MAXI J1828–294 from its discovery on October 15, 2013, to the end of February 2014 from the MAXI, SWIFT, and INTEGRAL data in different energy bands. The open circles represent the GSC/MAXI data (M) on the upper three panels and the BAT/SWIFT data (B) on the lower panel. The filled circles on the lower panel indicate the ISGRI/INTEGRAL data (I). The MAXI data points were obtained during  $\sim 1$  day of observations at energies  $< 10$  keV and three days at energies 10–20 keV; the ISGRI and BAT data points were obtained during 1 and 2 days, respectively; the actual MAXI and BAT exposure time often did not exceed a couple of hours.

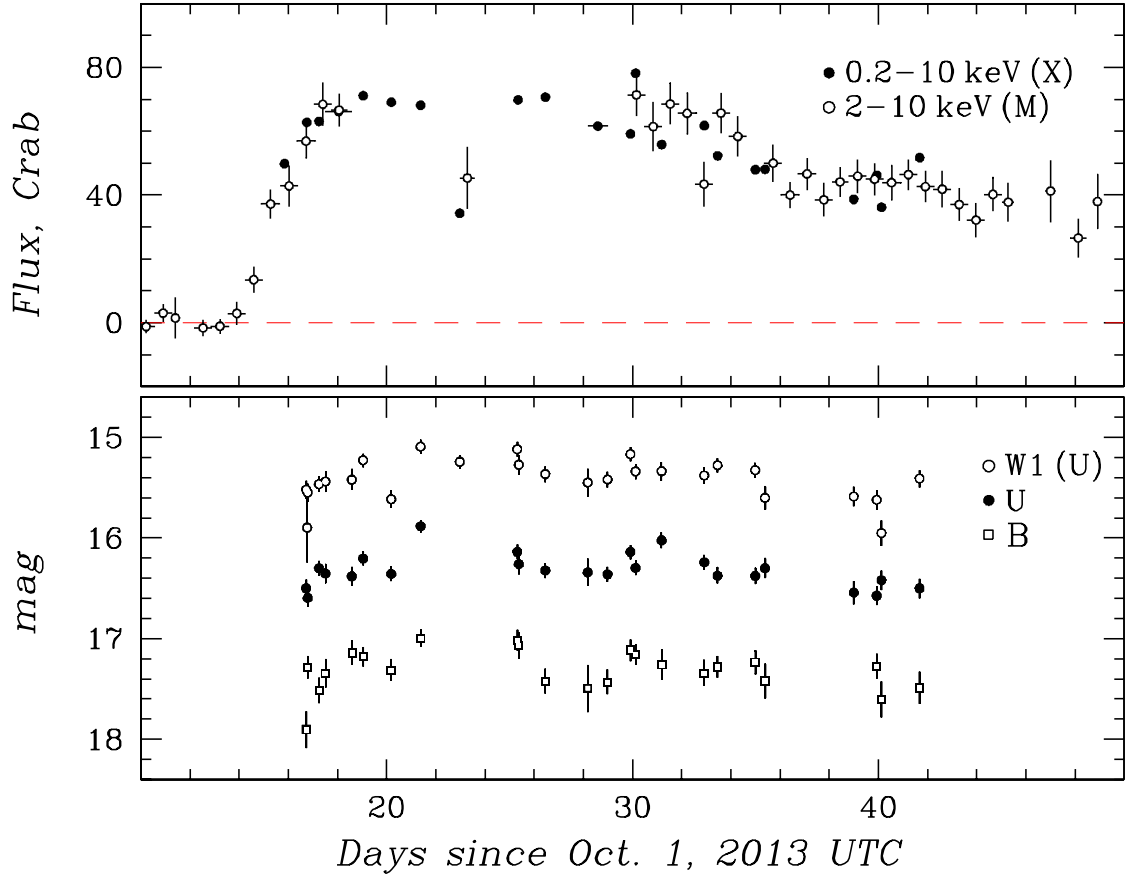


**Fig. 3:** Comparison of the soft X-ray ( $< 10$  keV) and OUV light curves for the initial stage of the outburst of MAXI J1828–249 (October — November 2013). The filled and open circles on the upper panel indicate the XRT/SWIFT (X) and GSC/MAXI (M) X-ray flux measurements, respectively; the UVOT/SWIFT (U) flux measurements in the W1, U, and B filters are shown on the lower panel. The W1 light curves is shifted by 1.2 mag upward for clarity. The resolution corresponds to about 18–24 h.

onset of the outburst and then continued to slowly decrease. Note that the SWIFT/XRT spectral measurements performed at this time (on February 14, 2014) showed that the source passed to a hard state and its X-ray 0.5–10 keV spectrum was described by a simple power law with a photon index of  $1.7 \pm 0.15$  (Tomsick and Corbel 2014). The first detection of radio emission from MAXI J1828–294 (Corbel 2014) also refers to this time. The radio source was detected with a flux density of  $\simeq 1.3$  mJy at 3.5 cm and had a flat spectrum suggesting a synchrotron origin and self-absorption.

The light curve in Fig. 3 (filled circles) shows the initial activity stage of the source in the 0.2–10 keV band. It was obtained by the XRT/SWIFT X-ray telescope with smaller errors and more complete coverage than those for the GSC/MAXI instrument (open circles, the 2–10 keV band). According to this light curve, the flux from the source reaches its

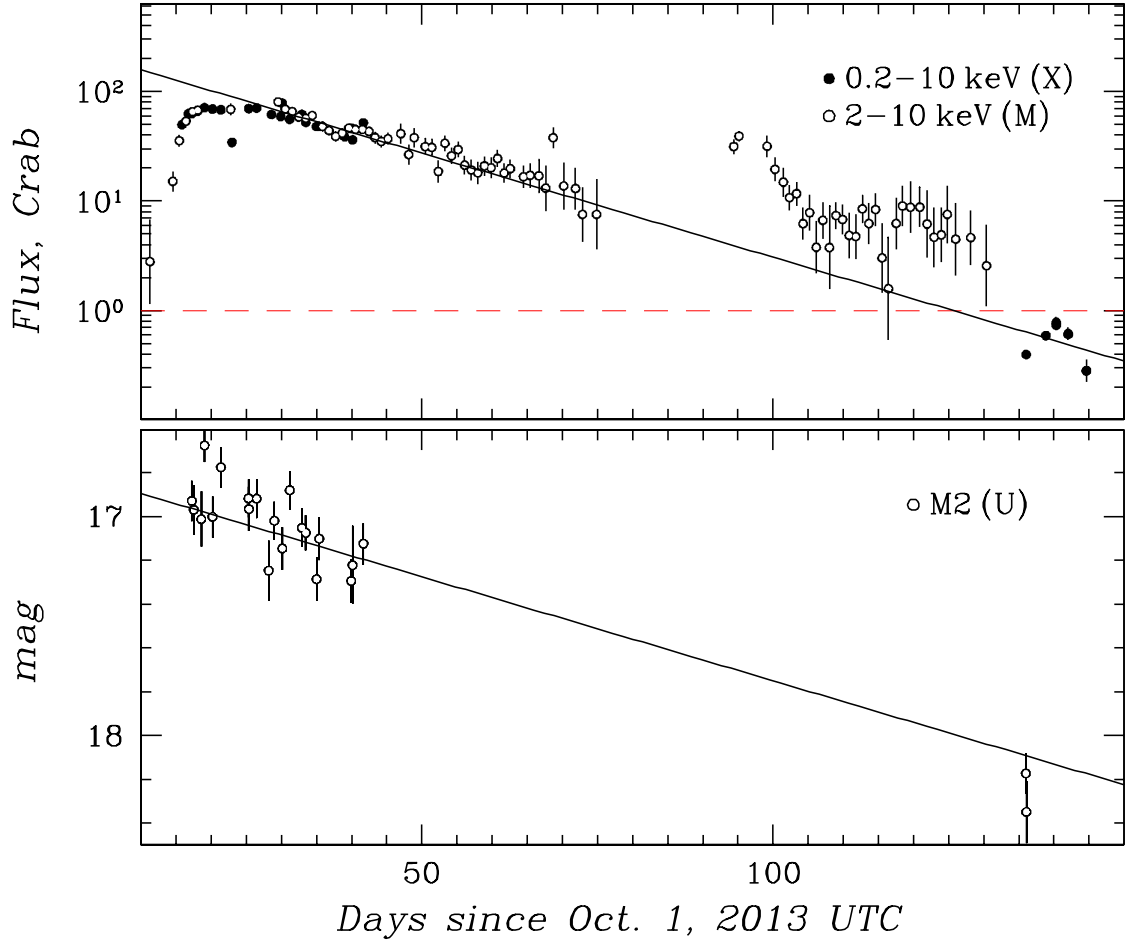


**Fig. 4:** Comparison of the long-term (October 2013 — February 2014) X-ray ( $< 10$  keV) and optical (M2 filter) light curves for MAXI J1828–249 from the data of the XRT (X) and UVOT (U) telescopes of the SWIFT observatory and the GSC instrument of the MAXI observatory (M).

maximum already by October 18 and then began to gradually decrease. The figure confirms the presence of the above dip in the light curve by  $\sim 50\%$  near October 25. The short ( $\sim 1$  day) spike in the light curve near October 30 is also of interest. The lower panel in the figure presents the optical and ultraviolet (U, B, and W1) light curves constructed from the UVOT/SWIFT measurements. The observed variability follows the soft X-ray variability in many details, suggesting that the OUV emission closely correlates with the X-ray one, i.e., it originates in the same region or is the result of its direct reprocessing under accretion disk irradiation. This can be seen even better from Fig. 4, which presents the same X-ray light curves but over a longer period (October 2013 — February 2014) in comparison with the UVOT M2 light curve. A logarithmic axis is used for the X-ray flux in this figure; the straight lines specify an exponential decay with the same decay time scale of  $\simeq 53$  days for the X-ray and optical bands. The flux in both bands is seen to actually decrease according



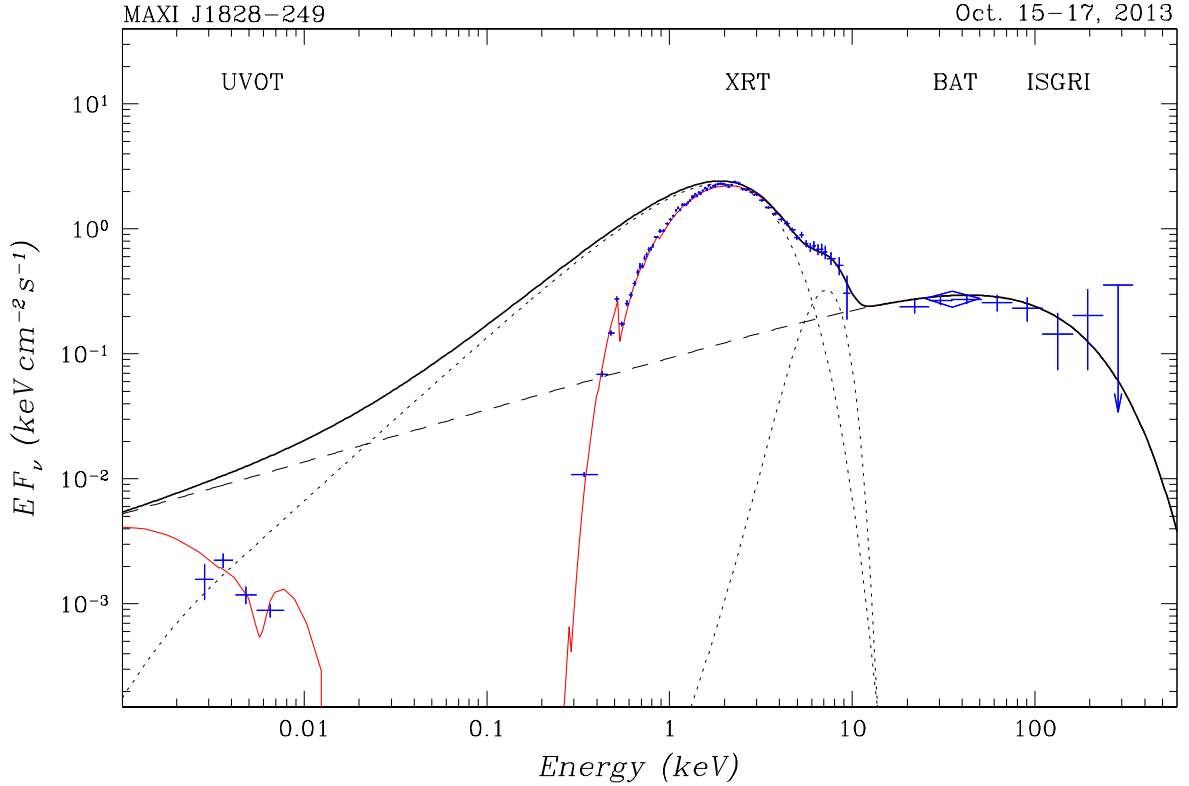


**Fig. 5:** Broadband (0.002–400 keV) spectrum of MAXI J1828–249 obtained by INTEGRAL and SWIFT on October 15–18, 2013. The thick solid (black) line indicates its fit by the adopted model (see the text); the thin solid (red) line represents the same model after the correction for interstellar absorption. The dashed line indicates the hard component of the spectral model connected with Comptonization (fitted by a power law with an exponential cutoff at high energies); the dotted lines indicate other components of the model: blackbody disk radiation and a Gaussian iron fluorescence line at 6.4 keV.

to a single law.

It is difficult to judge the shape and evolution of the source’s broadband spectrum from the light curves alone. It is necessary to have the spectrum itself at various outburst stages. To obtain such spectra, we selected seven time intervals with maximally wide energy coverage, from the optical to the hard X-ray bands, from all of the available data. The start (end) date and time of observations for the instruments operated in each interval are given in Table 1.

The source’s spectrum taken during the first interval of observations, on October 15–18, 2013, i.e., almost immediately after its discovery, is presented in Fig. 5. We used the quasi-simultaneous IBIS/ISGRI, BAT, XRT, and UVOT observations. The relative data normalization was set equal to unity for all instruments. The thin solid line indicates the best fit to this spectrum; the thick solid line indicates the same model spectrum corrected

**Table 1.** Measurements of the spectrum for MAXI J1828–249  
at various stages of its outburst<sup>a</sup>

Date	OIR & UV		0.4–10 keV	> 20 keV	
	RTT-150	UVOT	XRT	BAT	IBIS
2013					
Oct. 15–18		17 17 <sup>h</sup> 15 <sup>m</sup>	–''–	–''–	15 18 <sup>h</sup> 03 <sup>m</sup> –18 02 <sup>h</sup> 58 <sup>m</sup>
Oct. 18–20		20 00 <sup>h</sup> 55 <sup>m</sup>	–''–	–''–	18 21 <sup>h</sup> 55 <sup>m</sup> –20 09 <sup>h</sup> 13 <sup>m</sup>
Oct. 21–22		21 04 <sup>h</sup> 26 <sup>m</sup>	–''–	–''–	21 17 <sup>h</sup> 35 <sup>m</sup> –22 13 <sup>h</sup> 39 <sup>m</sup>
Nov. 9	15 <sup>h</sup> 42 <sup>m</sup>	22 <sup>h</sup> 14 <sup>m</sup>	–''–	–''–	
Nov. 10	15 <sup>h</sup> 52 <sup>m</sup>	02 <sup>h</sup> 50 <sup>m</sup>	–''–	–''–	
Nov. 11–12	12 15 <sup>h</sup> 45 <sup>m</sup>	11 16 <sup>h</sup> 01 <sup>m</sup>	–''–	–''–	
2014					
Feb. 13–14		13 23 <sup>h</sup> 59 <sup>m</sup>	–''–	–''–	14 13 <sup>h</sup> 45 <sup>m</sup> –17 <sup>h</sup> 26 <sup>m</sup>

<sup>a</sup> The start (end) date and time (UT) of the interval of observations.

The SWIFT and RTT-150 observations usually lasted  $\lesssim 1000$  s.

for interstellar absorption, i.e., the original spectrum of the source. The absorption was described by the fit from Morrison and McCammon (1981, the WABS code in XSPEC) in the low-energy part of the X-ray spectrum and by the REDDEN code, where the color correction  $E(B-V)$  was assumed to be equal to  $N_H/(5.6 \times 10^{21} \text{ cm}^{-2})$  (see Draine 2003), in the optical spectrum. Note once again that the measured  $N_H$  turned out to be very close to the average Galactic absorption expected in this direction,  $N_H \simeq (1.7 \pm 0.2) \times 10^{21} \text{ cm}^{-2}$  (Kalberla et al. 2005).

The dashed and dotted lines in the figure indicate the individual components of the spectral model used: (1) multicolor blackbody disk radiation (DISKBB in the XSPEC code; Shakura and Sunyaev 1973), (2) a power law with an exponential cutoff at high energies (CUTOFFPL in the XSPEC code), and (3) a Gaussian emission line to describe the iron fluorescence at 6.4 keV (GAUSSIAN). Note that the DISKBB model takes into account only the energy release due to viscous energy dissipation in the disk. The Gaussian line can also take into account possible excess emission formed in the transition region between the cold disk and the high temperature central cloud. The Gaussian line width was fixed at  $\sigma = 1.4$  keV, which roughly corresponds to the detector resolution. Other best-fit parameters and the corresponding luminosities are given in Table 2. When estimating the luminosity, we assumed MAXI J1828–249 to be near the Galactic center at a distance  $d \simeq 8$  kpc.

The spectrum of the blackbody disk presented in Fig. 5 was obtained by the integration over its surface from  $R_1 = 3R_g \simeq 9 \times 10^6 (M/10 M_\odot) \text{ cm} (= R_0)$  to  $R_2 = 1.5 \times 10^5 R_g \simeq 4.5 \times 10^{11} (M/10 M_\odot) \text{ cm}$  and, thus, was computed more accurately than in the DISKBB function<sup>2</sup>.

<sup>2</sup>In the DISKBB function of the XSPEC code, the integration is from the radius corresponding to the maximum disk temperature to infinity; therefore, if the blackbody disk extends sufficiently close to the

**Table 2.** Fits to the radiation spectrum of MAXI J1828–249

Model	Date						
	Oct. 15–18, 2013	Oct. 18–20, 2013	Oct. 21–22, 2013	Nov. 9, 2013	Nov. 10, 2013	Nov. 11–12, 2013	Feb. 13, 2014
Power-law model with exponential cutoff							
$N_{\text{H}}^{\text{a}}$	2.05±0.03	2.11±0.03	1.93±0.03	2.00±0.03	2.09±0.03	1.93±0.03	2.25±0.24
$\alpha_{\text{e}}$	1.60±0.02	1.69±0.01	1.63±0.01	1.42±0.01	1.44±0.01	1.43±0.01	1.73±0.05
$E_{\text{br},}$	108±27	139±41	93±21	20	20	17.3±2.8	150
$I_0,$	0.84±0.06	1.02±0.06	1.08±0.07	2.28±0.08	2.05±0.07	2.05±0.12	0.19±0.01
$kT_{\text{bb}}^{\text{e}}$	779±5	822±4	775±5	659±6	685±6	681±6	-
$R_{\text{bb}}\sqrt{\cos i}^{\text{f}}$	24.8±0.3	24.9±0.3	28.4±0.3	27.1±0.5	26.3±0.5	27.3±0.4	-
$\xi_{\text{RTT}}^{\text{g}}$	-	-	-	0.79±0.06	0.80±0.05	0.88±0.05	-
$I_{6.4}^{\text{h}}$	15.5±2.2	6.6±2.0	5.2±2.4	-	-	-	-
$L_{\text{X}1}^{\text{S}}$	72.5±5.6	100.6±5.9	94.3±6.5	52.3±1.8	56.8±2.1	58.6±3.6	6.97±0.51
$L_{\text{X}1}^{\text{H1}}$	6.68±0.52	6.80±0.40	6.97±0.40	-	-	-	1.81±0.13
$L_{\text{X}1}^{\text{H2}}$	2.29±0.18	2.20±0.13	2.53±0.17	3.01±0.11	2.46±0.09	2.00±0.12	0.43±0.03

<sup>a</sup> Hydrogen column density,  $10^{21} \text{ cm}^{-2}$ .

<sub>e</sub> Photon index.

<sub>e</sub> Energy of the high energy cutoff, keV.

<sub>e</sub> Normalization of the power-law spectral component,  $10^{-1} \text{ phot cm}^{-2} \text{ s}^{-1} \text{ keV}^{-1}$ .

<sup>e</sup> Temperature of the disk at its inner edge, eV.

<sup>f</sup> Inner radius of the disk assuming  $d = 8 \text{ kpc}$  ( $i$  — disk inclination), km.

<sup>g</sup> Relative normalization of the RTT-150 telescope data.

<sup>h</sup> Intensity of the 6.4 keV line,  $10^{-3} \text{ phot cm}^{-2} \text{ s}^{-1}$ .

<sub>1</sub> Luminosity in the energy ranges 0.001–13 (S), 13–400 (H1) and 25–50 (H2) keV assuming  $d = 8 \text{ kpc}$  after correction for photoabsorption,  $10^{36} \text{ erg s}^{-1}$ .

Such a spectrum describes the soft component in the X-ray spectrum appreciably better than is done by the DISKBB function. Here and below,  $R_{\text{g}} = 2GM/c^2$  is the gravitational radius of the black hole and  $M \simeq 10 M_{\odot}$  is its mass. The chosen outer disk radius  $R_2$  corresponds to the separation between the components of the binary system with a period of  $\sim 10 \text{ h}$ , typical of many X-ray novae (see, e.g., Cherepashchuk 2013). Restricting the disk size leads to a cutoff of its blackbody spectrum in the far infrared (Fig. 5).

It can be seen from Fig. 5 that at energies below  $\sim 25 \text{ eV}$ , the observed spectrum of the source within this model is dominated by a power-law emission component that exceeds the flux due to viscous energy dissipation in the outer disk regions by almost an order of magnitude. It is believed that the X-ray emission from the inner disk regions can be intercepted by the outer regions and, being reprocessed in them, can raise the disk surface

---

center, to (or almost to) the radius of the innermost stable orbit  $R_0 = 3 R_{\text{g}}$ , then the radiation from the innermost region, where the surface temperature already drops below the maximum one, turns out to be disregarded.

temperature. The OIR emission from the system must increase accordingly. This effect should be included in our analysis. The flux reradiated by a disk surface unit in the infrared and optical ranges is given by the equation (Shakura and Sunyaev 1973; Lyuty and Sunyaev 1976)

$$Q_{\text{irr}} = \frac{L_X (1 - \beta_d)}{4 \pi R^2} \left( \frac{H}{R} \right)^m \left( \frac{d \ln H}{d \ln R} - 1 \right). \quad (1)$$

Here,  $H \sim R^\gamma$  is the disk half-thickness at a given radius,  $\beta_d \simeq 0.9$  is the X-ray albedo of its surface (which take into account the fact that the emission is incident at very small angles; see, e.g., de Jong 1996),  $m = 1$  if the inner disk region is puffed up by the thermal and secular instabilities and, therefore, radiates almost isotropically and  $m = 2$  if the emitting region has a flat surface. We will assume  $m = 1$ , because the X-ray heating obviously turns out to be insignificant at  $m = 2$ . Comparison of  $Q_{\text{irr}}$  with the flux due to viscous energy dissipation in the disk (Shakura and Sunyaev 1973)

$$Q_{\text{vis}} = \frac{3}{8 \pi} \frac{G M \dot{M}}{R^3} \left[ 1 - \left( \frac{R_0}{R} \right)^{1/2} \right] \simeq \frac{3 L_d}{4 \pi R^2} \left( \frac{R_0}{R} \right)$$

shows that the X-ray heating of the disk surface dominates over the viscous one at distances  $R$  from the center exceeding the critical radius

$$R_{\text{irr}} \simeq \frac{30}{(\gamma - 1)} \left( \frac{L_d}{L_X} \right) \left( \frac{H}{R} \right)^{-m} R_0 \sim 36000 (L_d/L_X) R_0.$$

The regions near  $R_V \simeq 9600 (L_d/10^{38} \text{ erg s}^{-1})^{1/3} R_0 < R_{\text{irr}}$  mainly contribute to the optical (V filter) disk emission. Here,  $L_d \simeq 0.08 \dot{M} c^2 \gg L_X$  is the total energy release in the disk due to turbulent viscosity. It is clearly seen from Fig. 5 that the total luminosity of the hard power-law component ( $\simeq L_X$ ) is exceeded considerably, by a factor of 5–10, even by the luminosity of the blackbody accretion disk, which is lower than  $L_d$ . In the standard model of Shakura and Sunyaev (1973)  $H/R \simeq 6.7 \times 10^{-3} (R/R_0)^{1/8}$  ( $\gamma = 9/8$ ) depends weakly on  $R$ . The disk surface temperature in the heated region  $T_s = (Q_{\text{irr}}/\sigma + Q_{\text{vis}}/\sigma)^{1/4} \simeq (Q_{\text{irr}}/\sigma)^{1/4}$ , where  $\sigma$  is the Stefan-Boltzmann constant, decreases with radius as  $\sim R^{-1/2+m/32} \sim R^{-15/32}$  (see Eq. 1). In the disk region where the influence of surface heating is minor, the temperature decreases faster,  $T_s \sim R^{-3/4}$  (Shakura and Sunyaev 1973).

The solid lines in Fig. 6 indicate the spectra of such an X-ray-heated disk obtained for various  $L_X/L_d$  ratios by assuming the power-law component to undergo a break in the hard X-ray band (near  $\sim 1$  keV) and drops according to the Rayleigh-Jeans law at lower energies (virtually without contributing to the optical and infrared emissions from the system). From comparison with the power-law spectral component in Fig. 5 shown in this figure by long dashes we see that reradiation (X-ray disk surface heating) could actually explain the observed OIR emission from MAXI J1828–249, but only under the condition that  $L_X \gtrsim 5L_d$ ,

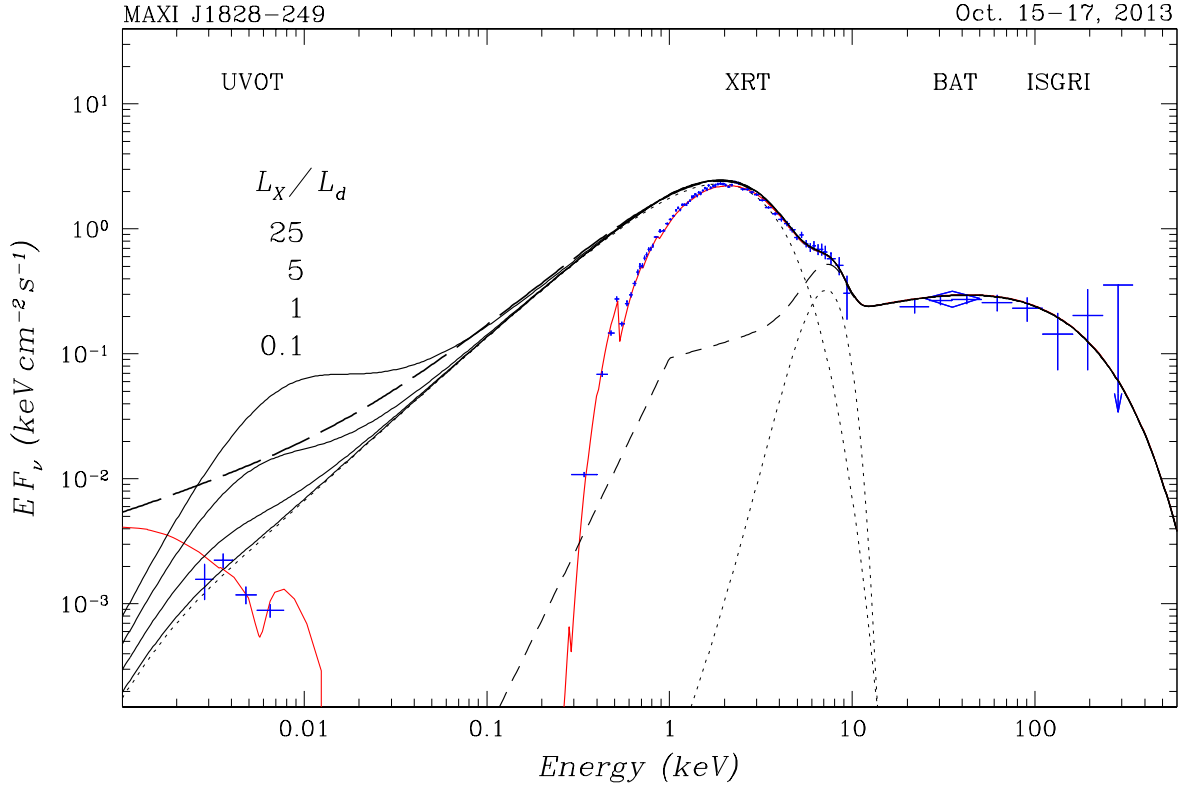


**Fig. 6:** The same broadband spectrum of MAXI J1828–249 obtained by INTEGRAL and SWIFT on October 15–18, 2013, as that in Fig. 5 but fitted by the model with a power-law component disappearing fast below 1 keV (dashed line with short dashes) that takes into account the irradiation of the multicolor blackbody accretion disk by hard emission from the central disk region (solid lines). Various possible ratios of the hard X-ray luminosity to the total disk luminosity,  $L_X/L_d = 25, 5, 1, 0.1$ , are considered. The dashed line with long dashes indicates the fit with the dominant contribution of a continuous power-law component (see Fig. 5).

i.e., in the presence of an additional intense central X-ray source. In the case of accretion onto a black hole, only the emission from the jets could be such a source that is scarcely probable. Figure 7 shows the spectrum with a dominant (in the optical band) power-law component, as in Fig. 5, but with a moderate (more realistic) contribution of the radiation from the heated disk, in accordance with  $L_X = 0.25L_d$ . Although the heating raises appreciably the optical and infrared disk luminosities, it is clearly insufficient to explain the observed optical emission from the system. Besides, the specific hard X-ray luminosity of this source during the observations being discussed was actually much lower than this value, as is clearly seen from comparison of the amplitudes of the hard and soft (blackbody) X-ray spectral components presented in Fig. 5 (the spectra are given in the form of  $E F_\nu$ , where  $F_\nu$  is the radiation spectrum; therefore, their amplitudes are proportional to the luminosity in the logarithmic scale of the figure) and the estimates of the source’s luminosity in the soft and hard bands presented in Table 2.

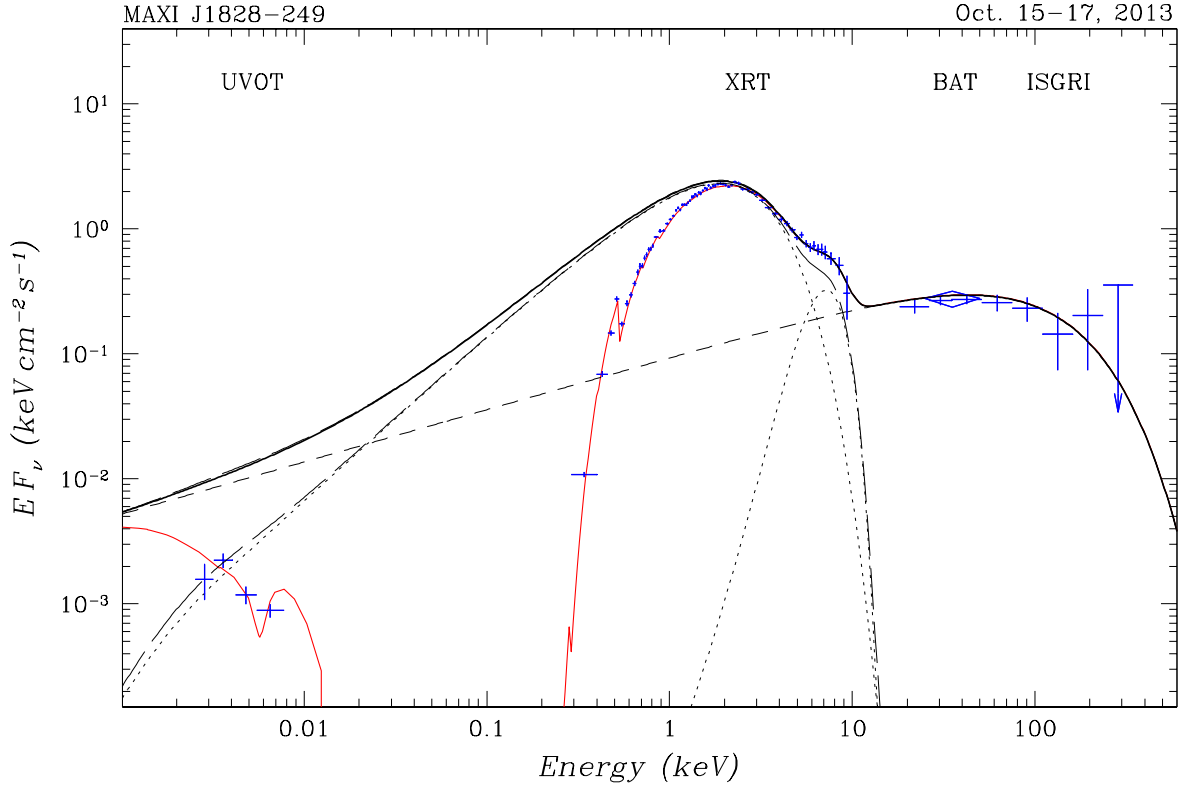


**Fig. 7:** The same broadband spectrum of MAXI J1828–249 obtained by INTEGRAL and SWIFT on October 15–18, 2013, as that in Fig. 5 but fitted by the model that takes into account the irradiation of the multicolor blackbody accretion disk by hard emission from its central region at  $L_X \simeq 0.25 L_d$  (long dashes).

All of the broadband spectra measured near or immediately after the maximum light of the X-ray nova MAXI J1828–249 (corresponding to the first six intervals of observations) can be fitted in a similar way. The parameters of the spectra are given in Table 2. The increase in the slope of the power-law component during the first week of observations turned out to be not so dramatic as was suggested by Krivonos and Tsygankov (2013). In subsequent days the slope even slightly decreased (till  $\sim 1.4$ ) but returned to the initial value of  $\sim 1.7$  by February. Of course, the real hardness of the spectrum in the X-ray band depended not only on this slope but also on energy of the exponential cutoff decreasing with time. The location of the inner edge of the blackbody region of the disk established shortly after the outburst onset subsequently barely changed, while the temperature of the disk surface gradually decreased. The intensity of the iron fluorescent line also decreased rapidly; it was noticeable only within the first days after the outburst when the disk approached the black hole quite closely. Three spectra corresponding to different phases of the source’s evolution are shown in Fig. 8 in comparison with the model spectrum obtained during the first observation. The third spectrum shown in this figure was taken in February 2014 at the decaying phase of the outburst (the seventh time interval in Table 1). This spectrum differs

noticeably from the first six spectra, being a purely power-law one, without any signatures of the blackbody component.

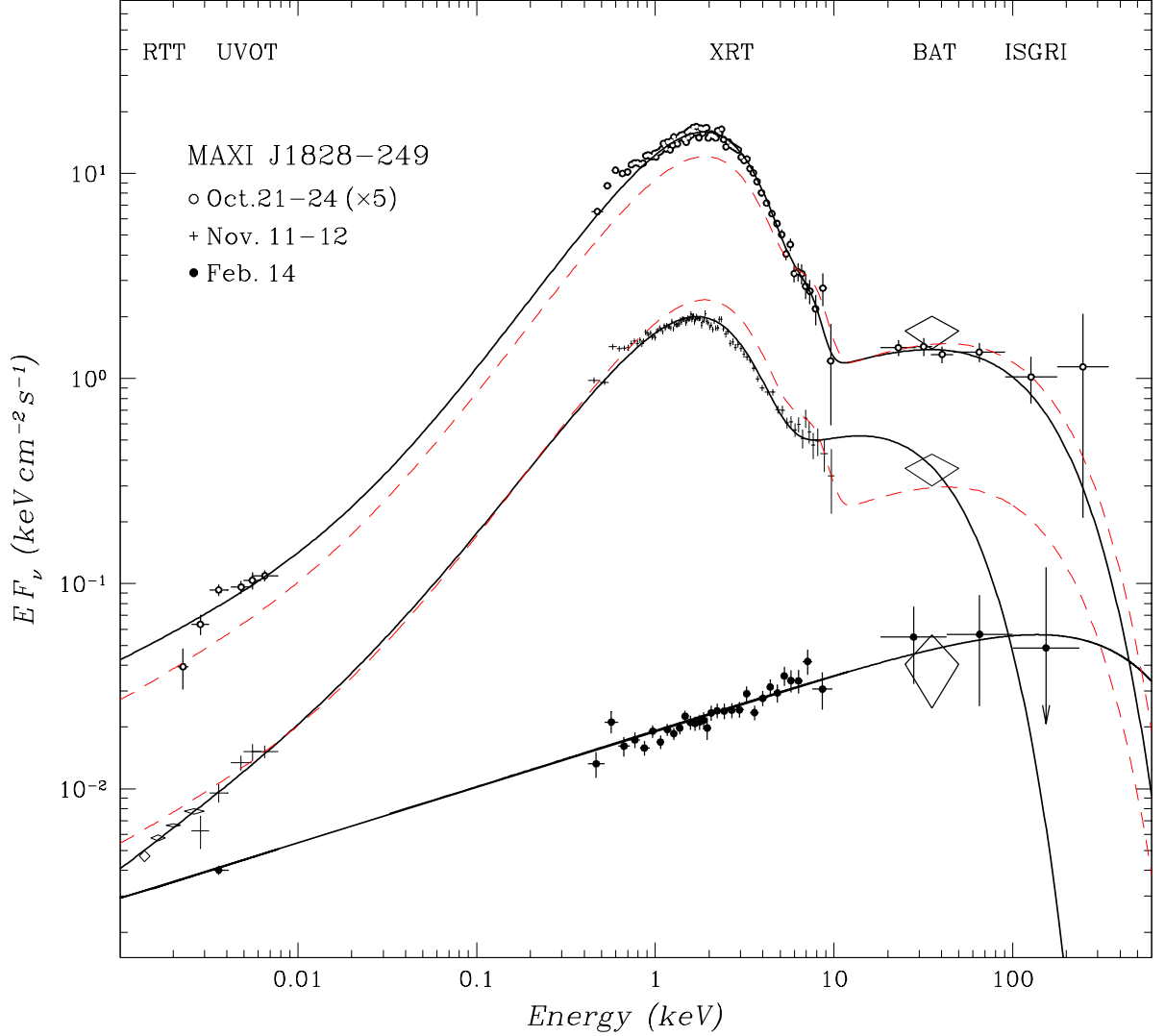


**Fig. 8:** Evolution of the broadband emission spectrum of the X-ray nova MAXI J1828–249 in October 2013 — February 2014 according to data from INTEGRAL (the ISGRI instrument) and SWIFT (BAT, XRT, and UVOT) observatories, and the RTT-150 telescope. The best-fit parameters are given in Table 2. The spectrum measured on October 21–24 is shifted for convenience upward by multiplying it by 5. For comparison, the dashed lines indicate the best-fit to the spectrum obtained during the first observation (on October 15–17, 2013).

## CONCLUSIONS

The results of our analysis of the INTEGRAL, SWIFT, MAXI, and RTT-150 observational data for the X-ray nova MAXI J1828–249 can be summarized as follows:

1. The ultraviolet, optical, and infrared emissions from the source during its 2013 outburst cannot be explained exclusively by the blackbody radiation from the distant outer accretion disk regions due to internal energy release and/or disk surface heating by hard photons emitted near the black hole. The blackbody radiation was weak both during the hard state of the source observed at the decaying phase of the outburst and during its soft (more likely two-component) state near the maximum of the X-ray flux from the nova.
2. The missing OIR emission from the source can be successfully explained by extrapolating to this spectral range the power-law emission component responsible for the hard power-law “tail” with an exponential cutoff at energies above  $\sim 100$  keV observed in the source’s spectrum.
3. The optical variability of the source as a whole coincided with the X-ray one on a time scale of days and weeks, confirming the conclusion about a unified spectrum.

## ACKNOWLEDGMENTS

This work is based on the data from the INTEGRAL observatory retrieved through its Russian and European Science Data Centers, the SWIFT observatory retrieved through NASA/HEASARC, the MAXI experiment onboard the ISS retrieved through the site MAXI.RIKEN.JP/TOP, and the 1.5-m RTT-150 telescope. We take the opportunity to thank the TUBITAK National Observatory (Turkey), the Space Research Institute of the Russian Academy of Sciences, and the Kazan Federal University for their support in using this telescope.

This study was financially supported by the Program of the President of the Russian Federation for Support of Leading Scientific Schools (project NSh-6137.2014.2). S.A. Grebenev is grateful to the Russian Foundation for Basic Research (project no. 13-02-01375-a) for its support, A.V. Mescheryakov is grateful for the support to the State Program for Increasing the Competitiveness of the Kazan Federal University.



## REFERENCES

1. R.A. Arnaud, in Proc. of the ASP Conf. Ser. 101 “Astronomical Data Analysis Software and Systems V”, Eds. G. Jacoby and J. Barnes (ASP, San Francisco, 1996), p. 17.
2. S.D. Barthelmy, L.M. Barbier, J.R. Cummings, E.E. Fenimore, N. Gehrels, D. Hullinger, H.A. Krimm, C.B. Markwardt, et al., Space Sci. Rev. **120**, 143 (2005).
3. D.N. Burrows, J.E. Hill, J.A. Nousek, J.A. Kennea, A. Wells, J.P. Osborne, A.F. Abbey, A. Beardmore, et al., Space Sci. Rev. **120**, 165 (2005).
4. S. Chaty, C.A. Haswell, J. Malzac, R.I. Hynes, C.R. Chr  der, and W. Cui, Mon. Not. Roy. Astron. Soc. **346**, 689 (2003).
5. A.M. Cherepashchuk, *Close Binary Stars* (Fizmatlit, Moscow, 2013) [in Russian].
6. S. Corbel, J.A. Tomsick, and T. Tzioumis, Astron. Tel. No. 5911 (2014).
7. J.A. de Jong, J. van Paradijs, and T. Augusteijn, Astron. Astrophys. **314**, 484 (1996).
8. B.T. Draine, Ann. Rev. Astron. Astrophys. **41**, 241 (2003).
9. P.A. Evans, R. Willingale, J.P. Osborne, P.T. O’Brien, K.L. Page, C.B. Markwardt, S.D. Barthelmy, A.P. Beardmore, et al., Astron. Astrophys. **519**, A102 (2010).
10. E. Filippova, E. Kuulkers, C. Sanchez-Fernandez, J. Wilms, V. Grinberg, M. Cadolle-Bel, J. Chenevez, R. Wijnands, et al., Astron. Tel. No. 5476 (2013).
11. N. Gehrels, G. Chincarini, P. Giommi, K.O. Mason, J.A. Nousek, A.A. Wells, N.E. White, S.D. Barthelmy, et al., Astrophys. J. **611**, 1005 (2004).
12. S.A. Grebenev, R.A. Sunyaev, and M.N. Pavlinsky, Adv. Space Res. **19**, 15 (1997).
13. S.A. Grebenev, A.V. Prosvetov, and R.A. Sunyaev, Astron. Lett. **39**, 367 (2013).
14. S.A. Grebenev, A.V. Prosvetov, and R.A. Burenin, Astron. Lett. **40**, 171 (2014).
15. P.M.W. Kalberla, W.B. Burton, D. Hartmann, A.M. Arnal, E. Bajaja, R. Morras, and W.G.L. P  ppel, Astron. Astrophys. **440**, 775 (2005).
16. J.A. Kennea, M. Linares, H.A. Krimm, P.A. Evans, P. Romano, V. Mangano, P. Curran, K. Yamaoka, and H. Negoro, Astron. Tel. No. 5478 (2013a).
17. J.A. Kennea, M. Linares, H.A. Krimm, P.A. Evans, P. Romano, V. Mangano, P. Curran, K. Yamaoka, and H. Negoro, Astron. Tel. No. 5479 (2013b).
18. R. Krivonos, and S. Tsygankov, Astron. Tel. No. 5492 (2013).
19. (R. Krivonos, M. Revnivtsev, S. Tsygankov, S. Sazonov, A. Vikhlinin, M. Pavlinsky, E. Churazov, and R. Sunyaev, Astron. Astrophys. **519**, A107 (2010).
20. F. Lebrun, J.P. Leray, P. Lavocat, J. Cr  tolle, M. Arqu  s, C. Blondel, C. Bonnin, A. Bou  re, et al., Astron. Astrophys. **411**, L141 (2003).

21. N. Lund, C. Budtz-Jorgensen, N.J. Westergaard, S. Brandt, I.L. Rasmussen, A. Hornstrup, C.A. Oxborrow, J. Chenevez, et al., *Astron. Astrophys.* **411**, L231 (2003).
22. V.M. Lyutyi and R.A. Sunyaev, *Sov. Astron.* **20**, 290 (1976).
23. M. Matsuoka, K. Kawasaki, S. Ueno, H. Tomida, M. Kohama, M. Suzuki, Y. Adachi, M. Ishikawa, et. al., *Publ. Astron. Soc. Japan* **61**, 999 (2009).
24. T. Mihara, M. Nakajima, M. Sugizaki, M. Serino, M. Matsuoka, M. Kohama, K. Kawasaki, H. Tomida, et. al. *Publ. Astron. Soc. Japan* **63**, S623 (2011).
25. J.C.A. Miller-Jones, *Astron. Tel. No.* 5484 (2013).
26. R. Morrison and D. McCammon, *Astrophys. J.* **270**, 119 (1983).
27. S. Nakahira, H. Tomida, H. Negoro, M. Morii, T. Mihara, S. Ueno, M. Kimura, M. Ishikawa, et al., *Astron. Tel. No.* 5474 (2013).
28. H. Negoro, M. Sugizaki, T. Mihara, M. Matsuoka, S. Nakahira, S. Ueno, H. Tomida, M. Kimura, et al., *Astron. Tel. No.* 5483 (2013).
29. J. Poutanen and A. Veledina, *Space Sci. Rev.* **183**, 61 (2014).
30. R.A. Remillard, J.E. McClintock, *Ann. Rev. Astron. Astrophys.* **44**, 49 (2006).
31. M.G. Revnivtsev, R.A. Sunyaev, D.A. Varshalovich, V.V. Zheleznyakov, A.M. Cherepashchuk, A.A. Lutovinov, E.M. Churazov, S.A. Grebenev, and M.R. Gilfanov, *Astron. Lett.* **30**, 382 (2004).
32. P.W.A. Roming, T.E. Kennedy, K.O. Mason, J.A. Nousek, L. Ahr, R.E. Bingham, P.S. Broos, M.J. Carter, et al., *Space Sci. Rev.* **120**, 95 (2005).
33. N.I. Shakura and R.A. Sunyaev, *Astron. Astrophys.* **24**, 337 (1973).
34. R.A. Syunyaev, I.Yu. Lapshov, S.A. Grebenev, V.V. Efremov, A.S. Kaniovskii, D.K. Stepanov, S.N. Yunin, E.A. Gavrilova, et al., *Sov. Astron. Lett.* **14**, 327 (1988).
35. R. Syunyaev, V. Aref'ev, K. Borozdin, M. Gil'fanov, V. Efremov, A. Kaniovskii, E. Churazov, E. Kendziorra, et al., *Sov. Astron. Lett.* **17**, 413 (1991).
36. Y. Tanaka and N. Shibasaki, *Ann. Rev. Astron. Astrophys.* **34**, 607 (1996).
37. J.A. Tomsick and S. Corbel, *Astron. Tel. No.* 5886 (2014).
38. P. Ubertini, F. Lebrun, G. Di Cocco, A. Bazzano, A. J. Bird, K. Broenstad, A. Goldwurm, G. La Rosa, et al., *Astron. Astrophys.* **411**, L131 (2003).
39. C. Winkler, T.J.-L. Courvoisier, G. di Cocco, N. Gehrels, A. Giménez, S. Grebenev, W. Hermsen, J.M. Mas-Hesse, F. Lebrun, et al., *Astron. Astrophys.* **411**, L1 (2003).